Qualitative Study of Substituent Effects on NMR ^{15}N and ^{17}O Chemical Shifts

Rubén H. Contreras,[†] Tomás Llorente,[†] Gabriel I. Pagola,[†] Manuel G. Bustamante,[†] Enrique E. Pasqualini,[‡] Juan I. Melo,[†] and Cláudio F. Tormena*[,§]

Department of Physics, FCEyN, University of Buenos Aires and CONICET, Buenos Aires, Argentina, Argentine National Atomic Energy Commission, Buenos Aires Province, Argentina, and Organic Chemistry Department, Chemistry Institute, University of Campinas, P.O. Box 6154; zip code 13084-971, Campinas, São Paulo, Brazil

Received: March 2, 2009; Revised Manuscript Received: July 22, 2009

A qualitative approach to analyze the electronic origin of substituent effects on the paramagnetic part of chemical shifts is described and applied to few model systems, where its potentiality can be appreciated. The formulation of this approach is based on the following grounds. The influence of different inter- or intramolecular interactions on a second-order property can be qualitatively predicted if it can be known how they affect the main virtual excitations entering into that second-order property. A set of consistent approximations are introduced in order to analyze the behavior of occupied and virtual orbitals that define some experimental trends of magnetic shielding constants. This approach is applied first to study the electronic origin of methyl−β substituent effects on both ^{15}N and ^{17}O chemical shifts, and afterward it is applied to a couple of examples of long-range substituent effects originated in charge transfer interactions such as the conjugative effect in aromatic compounds and σ-hyperconjugative interactions in saturated multicyclic compounds.

1. Introduction

Many years ago, Karplus, Pople et al.[1] presented a qualitative analysis of the paramagnetic part of magnetic shielding constants, which provided important insight into molecular factors defining several experimental trends. At present, although it is known that accurate calculations of nuclear magnetic shielding constants, σ, pose an important challenge to quantum chemistry methods,[2] very accurate calculations are known, as reported annually by Jameson and de Dios in the Specialist Periodical Reports series published by the Royal Society of Chemistry.[3] Despite such important advances that took place in the σ theoretical calculation, a qualitative analysis of these parameters is still quite appealing, especially for graduate students and for beginners in the application of NMR spectroscopy to study various molecular problems. It is expected that it could also be useful for most practitioners to obtain insight into the influence of intra- or intermolecular interactions originating σ experimental trends. For these reasons, care is taken to compare trends deduced from this qualitative model with actual σ DFT-GIAO calculations carried out on some simple model compounds. This calculation methodology is chosen because, at present, it is by far the most commonly used in recent literature to complement chemical shift measurements in experimentally oriented scientific papers.

It is important to highlight that this qualitative analysis is only valid for a second-order property, and therefore it can be applied to study the paramagnetic part but not to the diamagnetic part of the nuclear magnetic shielding tensor. This qualitative analysis is based on the comprehension of how occupied and virtual orbitals ("virtual excitations") respond to either intra- or intermolecular interactions. If an adequate physical understanding of such a response is achieved, then it is not difficult to get insight on how a second-order property behaves under such interactions. This analysis could start directly by a careful physical description of paramagnetic Hamiltonians, but it is easier to follow this reasoning if, as a starting point, a second-order perturbation expression is used. In the present case, the polarization propagator (PP), formalism corresponding to the paramagnetic part of the nuclear magnetic shielding tensor, is adopted, which is considered within the random phase approximation (RPA), because it is invariant under unitary transformations applied to canonical molecular orbitals. However, it should be noted that this approximation is by no means employed here to carry out calculations of the paramagnetic part of magnetic shielding constants. The qualitative approach discussed in this work is similar to that applied previously[4] for rationalizing trends of substituent effects on one- and two-bond nuclear spin−spin coupling constants.

In section 2, several characteristics of the nuclear magnetic shielding tensor, $\vec{\sigma}$ are discussed and the RPA PP expression for its paramagnetic part[5] is described briefly. Afterward, a set of consistent approximations are introduced into such an expression in order to get insight into how orbital interactions affect occupied and virtual orbitals appearing in second-order properties based on the Hartree−Fock method.

In section 3 are presented DFT calculations for $\vec{\sigma}$ tensors carried out on a series of model compounds where experimental methyl−β substituent effects either on $\sigma(^{15}N)$[6] or $\sigma(^{17}O)$[7] constants are known. Results thus obtained are discussed in terms of the qualitative model presented in section 2. Finally, conjugative and hyperconjugative long-range substituent effects in a few larger systems are discussed in terms of this qualitative approach.

2. The Nuclear Magnetic Shielding Tensor $\vec{\sigma}$(M)

This is a nonsymmetric second rank tensor, which, as it happens with all nonsymmetric second rank tensors, can be

* E-mail: tormena@iqm.unicamp.br.
[†] University of Buenos Aires and CONICET.
[‡] Argentine National Atomic Energy Commission, Buenos Aires Province.
[§] University of Campinas.

10.1021/jp901926p CCC: $40.75
Published on Web 08/17/2009

TABLE 1: Comparison of Basis Set Performance within the DFT-B3LYP Approach for Calculating the Magnetic Shielding Constant $\sigma(^{15}N)$ (in ppm) in Methyl- and Ethylamine

	DFT-linear response[a]			GIAO[b]
basis set	diamagnetic	paramagnetic	total	total
		Methyl-A[c]		
6-311G**	397.3629	−174.0190	223.3439	243.9137
Huz-III	397.0409	−162.4723	234.5686	235.9172
Huz-IV	397.0378	−160.8847	236.1531	236.0697
		Ethyl-A[c]		
6-311**	425.4638	−213.0658	212.3980	223.4530
Huz-III	425.1689	−210.9691	214.1999	214.8138
Huz-IV	425.1695	−210.1098	215.0597	215.0505

[a] Calculations carried out with the Dalton program.[16] [b] Calculations carried out with the Gaussian 03 program.[11] [c] A stands for amine.

decomposed into symmetric and antisymmetric contributions. The latter affects only the relaxation time but does not affect the magnetic shielding constant, σ(M), and consequently, for the purpose of this work, it will not be taken into account. For this reason, only the symmetric part will be discussed, although it will not be mentioned explicitly. Within the Ramsey nonrelativistic approach[8] the $\bar{\bar{\sigma}}$(M) tensor is composed of diamagnetic and paramagnetic parts, the former being a "first-order" quantity while the latter is a "second-order" one. The approach sought in this work is intended to be used as a complementary tool to experimental work to get insight into the electronic molecular structure when chemical shifts are reported in a series of compounds together with theoretical calculations of such parameters. For this reason, actual calculations presented in this work are carried out with the most commonly used method in such types of scientific papers. A brief perusal of the current literature shows that such a method is based on the GIAO−DFT (gauge-including atomic orbitals[9]-density functional theory) approach, and consequently this is adopted here. It is noted that there are in the literature several other alternative methods to calculate magnetic shielding tensors which are gauge-origin-independent.[10] The advantage of such approaches in comparison with the GIAO approach is that diamagnetic and paramagnetic parts can be calculated separately, but they are much less employed in the current literature.

In this work, σ(M) calculations are carried out within the DFT (density functional theory) framework, employing the Gaussian 03 program.[11] Besides, the B3LYP[12] functional is adopted because in many cases from the recent literature the results correctly describe experimental trends. The selection of an adequate basis set was made, trying one basis set of Pople's type, i.e., 6-311G**,[13] and two basis sets of Huzinaga's type, i.e., Huz-III and Huz-IV.[14] The following criterion was applied to choose one basis set considered satisfactory for the present purpose. In methyl- and ethylamine $\sigma(^{15}N)$ isotropic diamagnetic and paramagnetic parts were calculated separately, the former as a first-order quantity, the latter, within the DFT-linear response approach[15] using a common gauge origin. Such calculations were carried out using the Dalton program.[16] As displayed in Table 1, for the Huz-IV basis set both the common gauge-origin DFT linear response and the GIAO isotropic $\sigma(^{15}N)$ constants for both methyl- and ethylamine agree within 0.1 ppm. This agreement is taken as evidence that the Huz-IV basis set is good enough for the purpose of this work. It is highlighted that, as expected, the diamagnetic part is less sensitive to the basis set quality than the paramagnetic contribution. It is noted

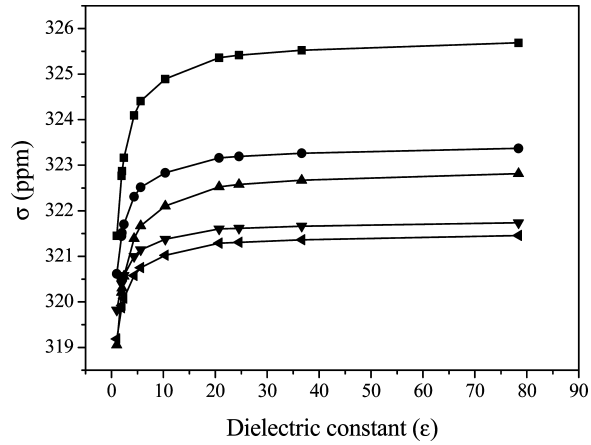

Figure 1. $\sigma(^{17}O)$ (in ppm) for dimethyl ether versus the solvent dielectric constant for different basis sets, calculated within the GIAO−DFT-B3LYP-X//B3LYP-6-311G** level, where *X*: ■ 6-311G**; ●: 6-311G(3d,3p); ▲: Huz-II; ▼: Huz-III; left-pointed triangle: Huz-IV.

that similar results were also obtained for the ^{17}O magnetic shielding constant in dimethyl ether, although they are not shown explicitly here.

It is often accepted that substituent effect trends are mainly determined by the paramagnetic part of magnetic shielding tensors. Results displayed in Table 1 show that the diamagnetic part of $\sigma(^{15}N)$ in methyl- and ethylamine are also affected by substituent effects. However, the methyl substituent effect on the diamagnetic part corresponds to a shielding effect, while that on the paramagnetic part corresponds to a deshielding effect, i.e., the experimental trend is given by that of the paramagnetic term (vide infra).

Because both $\sigma(^{15}N)$ and $\sigma(^{17}O)$, in general, depend on solvent,[17,18] in Figure 1 is plotted $\sigma(^{17}O)$ in dimethyl ether vs the solvent dielectric constant, for different basis sets, calculated within the GIAO−DFT approach. In all cases the geometry is optimized at the DFT-B3LYP/6-311G** level, taking into account the respective dielectric constant. Dielectric solvent effects are taken into account using the Polarizable Continuum Model of Tomasi et al.[19]

It is observed that the calculated $\sigma(^{17}O)$ in dimethyl ether is less sensitive to dielectric solvent effects as the quality of the basis set employed in its calculation improves. It is also observed in Figure 1 that, for all basis sets, there is a saturation of the dielectric solvent effect for $\varepsilon \sim 20$. It is recalled that a similar saturation of the dielectric solvent effect was observed for calculations of $^1J_{CC}$ nuclear spin−spin coupling constants for $\varepsilon \sim 10$ in aromatic compounds.[20] This saturation of solvent effects is observed when dielectric models are used because of the dependence of the solvent energy on the ratio $(\varepsilon - 1)/(\varepsilon + 2)$.[21]

The qualitative approach discussed in the next section is expected to yield insight into how substituent effects affect the $\bar{\bar{\sigma}}$(M) eigenvalues. This describes the convenience of briefly analyzing how eigenvalues depend on the basis set used for carrying out their calculation. For this purpose, a coordinate system, *X*, *Y*, *Z*, coinciding with the dimethyl ether eigenvectors is taken. The symmetry elements of this compound make it easy to determine such directions as shown in Figure 2. The dependence of eigenvalues on the basis set quality used in their calculations is displayed in Figure 3 for dielectric solvent constants $\varepsilon = 1$ (A) and $\varepsilon = 80$ (B).

In Figure 3 there is a "crossover" between two eigenvalues in dimethyl ether when increasing the size of the basis set. When

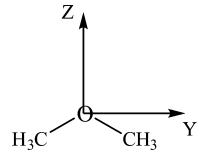

Figure 2. Eigenvectors of the $\vec{\sigma}(^{17}O)$ tensor in dimethyl ether, labeled *X*, *Y*, *Z*, are chosen to correspond to a right-handed coordinate system.

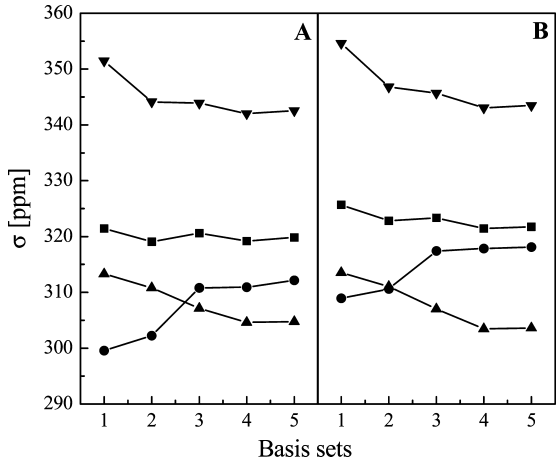

Figure 3. Dependence of $\sigma(^{17}O)$ eigenvalues (in ppm) in dimethyl ether vs the basis set size. ■: isotrope; ▲: *X*; ●: *Y*; ▼: *Z*. Basis sets: (1) 6-311G**; (2) Huz-II; (3) 6-311G(3d,3p); (4) Huz-III; (5) Huz-IV. (A) Calculations were carried out taking $\varepsilon = 1$; (B) as in A but considering $\varepsilon = 80$.

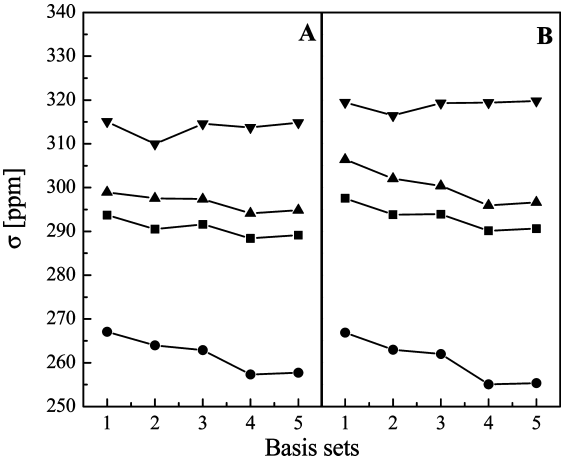

Figure 4. Basis set dependence of $\vec{\sigma}(^{17}O)$ eigenvalues in ethyl methyl ether (in ppm). ■: isotrope; ●: *X*; ▲: *Y*; ▼: *Z*. Basis sets: (1) 6-311G**; (2) Huz-II; 3) 6-311G(3d,3p), (4) Huz-III; (5) Huz-IV. (A) Calculations were carried out taking $\varepsilon = 1$, (B) as in A but considering $\varepsilon = 80$.

considering $\varepsilon = 80$, Figure 3B, this "crossover" is yet more notorious than for $\varepsilon = 1$. Changes in the basis set dependence for the different eigenvalues are highlighted.

In the optimized geometry of ethyl methyl ether the four heavier atoms are in a plane, which is a symmetry plane. Therefore, the perpendicular to that plane corresponds to a $\vec{\sigma}(^{17}O)$ tensor eigenvector, which is labeled *X* as in Figure 2 for dimethyl ether. In Figure 4 the three eigenvalues and the isotropic σ constant calculated with different basis sets, for $\varepsilon = 1$ (part A), and $\varepsilon = 80$ (part B), are displayed. A deshielding effect when going from dimethyl ether to ethyl methyl ether is observed when comparing the *X* eigenvalues in Figures 2 and 3. This effect is rationalized below in terms of the qualitative model discussed in the next section.

a. The Paramagnetic Part of the Nuclear Magnetic Shielding Tensor. To understand the qualitative analysis presented in this work, it is necessary to obtain insight into how molecular interactions affect Hartree−Fock virtual excitations. This is achieved taking a close look at the polarization propagator expression of the paramagnetic part of $\vec{\sigma}(M)$ taken at the RPA level, eq 1.[5,22]

$$\sigma_M^p = \Omega^\sigma \sum_{\alpha=1}^{3} \sum_{ia,jb} \{ U^p_{ia,\alpha} ({}^1A + {}^1B)^{-1}_{ia,jb} U^p_{jb,M\alpha} + U^p_{ia,M\alpha} ({}^1A + {}^1B)^{-1}_{ia,jb} U^p_{jb,\alpha} \} \quad (1)$$

where Ω^σ includes several constants, which are not described in detail because the approach presented here is only qualitative. α stands for a Cartesian component, i and j labels represent occupied molecular orbitals (MOs), a and b labels represent virtual MOs; $W_{ia,jb} = ({}^1A + {}^1B)^{-1}_{ia,jb}$ are the elements of the inverse of the singlet polarization propagator matrix $W_{ia,jb}$ involving the i→a and j→b virtual excitations, where

$${}^1A_{ia,jb} = (\varepsilon_a - \varepsilon_i)\delta_{ab}\delta_{ij} + 2\langle aj|ib\rangle - \langle aj|bi\rangle \quad (2)$$

$${}^1B_{ia,jb} = \langle ab|ji\rangle - 2\langle ab|ij\rangle \quad (3)$$

and the corresponding molecular bielectronic integrals are

$$\langle aj|ib\rangle = \int d^3r_1 d^3r_2 a^*(1) j^*(2) \frac{1}{r_{12}} b(1) i(2) \quad (4)$$

Besides,

$$U^p_{ia,\alpha} = \langle i|(\vec{R}\times\vec{\nabla})_\alpha|a\rangle \quad (5)$$

$$U^p_{jb,M\alpha} = \langle i|\left(\frac{\vec{R}_M\times\vec{\nabla}}{R_M^3}\right)_\alpha|b\rangle \quad (6)$$

are the Cartesian α components of the paramagnetic "perturbators", i.e., they are the (i,a) matrix elements of the paramagnetic perturbative Hamiltonians, where $\vec{R}$ and $\vec{R}_M$ stand for the electron position vector from the gauge origin and from the nucleus M site, respectively. For this qualitative analysis, the gauge origin is assumed to be taken at the site of nucleus M.

Because the RPA approximation is invariant under unitary transformations, in eqs 1−6 i and j can be assumed to represent occupied localized molecular orbitals (LMOs). Similarly, a and b can be thought to represent virtual LMOs, where it is assumed that the localization procedure is applied separately to occupied and virtual canonical orbitals obtained in a Hartree−Fock calculation. It is recalled that diagonal terms of the *W* matrix, i.e., those satisfying i = j and a = b, are its largest elements, and they are the only terms that depend explicitly on the energy gap, $\Delta = \varepsilon_a - \varepsilon_i$, corresponding to the i→a virtual excitation. From eq 1 changes in the paramagnetic shielding tensor along a series of compounds can be divided into factors affecting (1) the polarization propagator matrix elements and (2) the "perturbators"; of course, some molecular interactions could affect both of them.

TABLE 2: Eigenvalues of the DFT-GIAO-B3LYP-Huz-IV// B3LYP-6-311G ^{15}N Magnetic Shielding Tensors (in ppm) for Compounds 1 (NH_3), 2 (NH_2CH_3), and 3 ($NH_2CH_2CH_3$)**

eigenvalues	*X*	*Y*	*Z*	isotrope	$CH_3(\beta)$
NH_3	274.1	274.1	226.7	258.3	−
NH_2CH_3	261.1	241.9	205.2	236.1	22.2
$NH_2CH_2CH_3$	180.4	243.2	221.5	215.0	21.0

How are virtual excitations affected by inter- or intramolecular interactions? Because the pictorial representation sought in this work is only qualitative, it is expected that occupied and vacant LMOs behave approximately like natural bond orbitals (NBOs), as obtained by the method of Weinhold et al.[23] Orbital energies are also assumed to follow trends similar to NBO energies. Therefore, occupied and virtual LMOs are assumed to be affected by orbital interactions such as, for instance, conjugative and hyperconjugative interactions in a way similar to that of the corrresponding NBO orbitals. It is noted that at present the most commonly used approach to study electron delocalization interactions is Weinhold et al.'s NBO approach,[22] and, according to the well-known "perturbed molecular orbitals theory" (PMO),[24] the interaction between an occupied and a vacant LMO shifts, in energy, "downward" from the occupied orbital and "upward" from the vacant one. This means that conjugative or hyperconjugative interactions involving either the occupied or the vacant LMO of any virtual excitation will affect the corresponding PP term. This effect will be particularly important for PP diagonal terms because in such cases both pairs of occupied−vacant orbitals involved in a virtual excitation are affected by the hyperconjugative effect. The total influence on the corresponding sum in eq 1 will also depend on the significance of the corresponding "perturbator" terms. However, interactions such as the "inductive" effect could affect notably virtual excitations, although changes in the occupied and in the virtual orbital do not follow the PMO theory.

It is easy to qualitatively detect terms in eq 1 that are significant because in eqs 5 and 6, once the gauge origin is assumed to be taken at the site of nucleus M whose σ is under study, both of them involve, essentially, the 90° rotation operator through the α axis. Therefore, when rotating 90° an occupied LMO through that axis, it should show a significant overlap with an antibonding orbital for yielding in eq 1 an appreciable contribution, provided the corresponding PP term is also non-negligible. One of the "perturbators" depends on R^{-3}, and therefore it should correspond to a deshielding effect whenever the M atom is undergoing steric compression.[25] This effect was also taken into account by the simplified treatment presented by Karplus and Pople.[1] On the other hand, an attractive interaction, such as for instance a hydrogen bond, should yield a shielding effect on the hydrogen-bond acceptor.

3. Applications of the Qualitative Approach

a. Analysis of the Methyl−β Substituent Effect on the $\bar{\sigma}(^{15}N)$ Tensor in Ammonia (1), Methylamine (2), and Ethylamine (3). In Table 2 are displayed the DFT-GIAO $\bar{\sigma}(^{15}N)$ eigenvalues calculated at the B3LYP-Huz-IV//B3LYP-6-311G** level for compounds **1**, **2**, and **3**. In **1** it is very easy to identify the corresponding eigenvectors because this compound has a 3-fold symmetry axis, which must be one of its eigenvectors, and the other two must be any pair of perpendicular axes that are also orthogonal to the *Z* eigenvector, Figure 5, i.e., there is degeneration for eigenvalues corresponding to eigenvectors perpendicular to the 3-fold symmetry axis.

As mentioned above, the methyl substitution in compound **2** affects both the diamagnetic and the paramagnetic parts of the nuclear magnetic shielding tensor. However, they are affected in opposite directions, i.e., the diamagnetic part undergoes a shielding effect while the paramagnetic part undergoes a deshielding effect, i.e., the experimental trend of the isotropic part of that tensor is determined by the paramagnetic part. Therefore, the experimental trend can be rationalized in terms of the qualitative model described above. Besides, it is important to stress here that such a qualitative model cannot be applied to rationalize the diamagnetic trend because this is a first-order quantity.

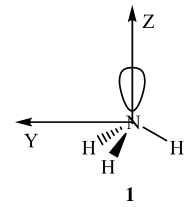

1

Figure 5. Eigenvectors in ammonia (**1**). The plane perpendicular to the *Z* axis presents degeneracy for both the corresponding eigenvectors and their corresponding eigenvalues.

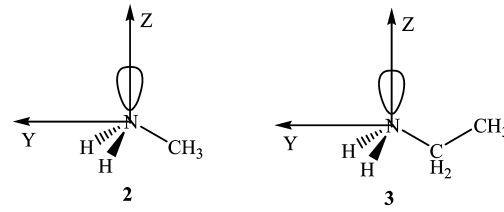

Figure 6. Approximate eigenvectors in compounds **2** and **3**. A right-handed Cartesian coordinate system is chosen.

TABLE 3: Five Relevant Energy Gaps for Defining the $\bar{\sigma}(^{15}N)$ Eigenvalues in 1, 2, and 3 (in Hartrees)

energy gap		**1**	**2**	**3**
Δ(**1**)	(N−H)*-LP(N)	0.784	0.752	0.753
Δ(**2**)	(C−N)*-LP(N)	−	0.670	0.642
Δ(**3**)	(N−H)*-(N−H)	1.068	0.941	1.047
Δ(**4**)	(N−H)*-(C−N)	−	1.148	1.141
Δ(**5**)	(N−C)*-(N−H)	−	0.828	0.934

For compounds **2** and **3**, eigenvectors are not the same as in **1**; however, they differ by only a few degrees as was also observed for a substituent close to a two-coordinated oxygen atom.[26] Because such small changes affect only slightly the overlap of a 90° rotated occupied LMO and a vacant one, in general they are much less important than the energy gaps defined, in the cases under consideration, by the inductive effect. Therefore, such changes are usually not very important for a qualitative description of the paramagnetic part of $\bar{\sigma}(^{15}N)$ in compounds **1**, **2**, and **3**. For this reason, eigenvalues shown in Table 2 can be assumed to have almost the same eigenvectors for all these three compounds, Figure 6. Therefore, it is possible to easily analyze their paramagnetic trends by applying the qualitative analysis described in section 2.

The relevant energy gaps, i.e., those corresponding to diagonal elements of the polarization propagator matrix that enter into the eigenvalues of the $\bar{\sigma}(^{15}N)$ magnetic shielding tensor, for compounds **1**, **2**, and **3** are displayed in Table 3.

Why in ammonia (**1**) is the *Z* eigenvalue smaller than the other two? The paramagnetic part of the *Z* eigenvalue is expected to have a larger absolute value than those of the *X* and *Y* eigenvalues. Only diagonal terms of the polarization propagator matrix are considered because they are the most important. For different occupied LMOs, if a 90° rotation around the *Z* axis is assumed, it is observed that the LP(N) is not affected because it is axially symmetric around the *Z* axis.

Therefore, the main contribution to the paramagnetic *Z* eigenvalue should originate in the overlap between a 90° rotated around the *Z* eigenvector N−H bonding and an (N−H)* antibonding orbital, with Δ(**3**), Table 3, as the relevant energy gap. Actually there are three equivalent terms of this type and are assumed to correspond to an important paramagnetic contribution to the *Z* eigenvalue because it is larger, in absolute value, than those for the *X* and *Y* eigenvalues, which involve the Δ(**1**) energy gap, but there is only one important contribution.

On the other hand, the *X* and *Y* $\vec{\sigma}(^{15}N)$ eigenvalues in **1**, **2**, and **3** should show a somewhat more complicated picture. When rotating an occupied LMO 90° around the *X* or *Y* axis, a non-negligible overlap between an occupied and a vacant LMO is expected for different vacant-occupied pairs. Some contain the energy gap $\Delta(\mathbf{1}) = \varepsilon_{(N-H)^*} - \varepsilon_{LP(N),}$ while others contain gaps defined by bonding and antibonding orbitals labeled Δ(**3**), Δ(**4**), and Δ(**5**), Table 3. It is recalled that these last two correspond to Δ(**1**) in **1**.

For rationalizing differences between the *Z* eigenvalues in **1**, **2**, and **3**, the main point should be to consider the energy gaps of types Δ(**3**), Δ(**4**), and Δ(**5**). On the other hand, for analyzing the *X* and *Y* eigenvalues, besides the energy gaps mentioned above, the Δ(**1**) and Δ(**2**) energy gaps should also be important. However, it is noted that a 90° rotated occupied molecular orbital around the different coordinate axes yield significantly different overlaps, although the corresponding energy gaps are the same. Comparing *Z* eigenvalues it is noted that in **1** there are three Δ(**3**) energy gaps while in compounds **2** and **3** there is only one Δ(**3**) energy gap, but the Δ(**4**) and Δ(**5**) are equivalent to Δ(**3**) for **1**. This comparison indicates that in **2** these gaps are notably smaller than in compound **1**, while in **3** this trend is reversed although the difference is not as significant as in Δ(**3**) and Δ(**5**). This trend is compatible with the *Z* eigenvalues trend displayed in Table 2 for compounds (**1**) and (**2**), i.e., the *Z* eigenvalue shows a deshielding effect when going from **1** to **2**. Comparing Δ(**3**) with Δ(5) energy gaps in compounds **2** and **3**, the *Z* eigenvalue in **3** must be notably larger than in **1** and **2**, corresponding to a shielding effect.

Applying similar considerations to the *X* and *Y* eigenvalues along compounds **1**, **2**, and **3**, it is observed in Table 2 that these trends are qualitatively described just by the energy gaps containing the lone pair. This could be expected on intuitive grounds because its occupied LMO corresponds to a very shallow orbital energy defining small energy gaps, and they correspond to deshielding effects.

As displayed in Table 2, the calculated methyl−β substituent effect in compounds **2** and **3** corresponds to a deshielding effect of about 21 ppm. This should be compared with the chemical shift difference, measured (with respect to nitromethane) using the same solvent and concentration (2 M in methanol) for both **2** (+377.3 ppm) and for **3** (+355.4 ppm), i.e., the difference is 21.9 ppm. (It is recalled that N chemical shifts are usually taken as positive for increasing magnetic fields.[6]) Results discussed above show that, by far, the main effect defining the methyl−β substituent effect originates in the inductive effect that decreases a pair of relevant energy gaps that define a deshielding effect. It should be noted that any hyperconjugative interaction transferring charge into the environment of the N atom, as discussed above from the PMO theory, would widen the relevant energy gaps, yielding a shielding effect opposite to that of the inductive effect.

b. Analysis of the Methyl−β Substituent Effect on the $\vec{\sigma}(^{17}O)$ Tensor in Dimethyl Ether (4) and in Ethyl Methyl Ether (5). The methyl substituent effect in (**4**) shows a behavior similar to that in (**2**), i.e., it yields a shielding effect on the diamagnetic part of the ^{17}O nuclear magnetic shielding constant, and a deshielding effect on the paramagnetic part, i.e., the paramagnetic part determines the experimental trend on the total shielding constant. Therefore, in this case the qualitative model described above can be used to rationalize the experimental trend. *X* is the only eigenvalue to be rationalized here for compounds **4** and **5** because the *Y* and *Z* eigenvectors in **5** depart notably from those in **4**. In Table 4 are shown such eigenvalues, together with the respective isotropic components, and the resulting methyl−β substituent effect. The larger *X* eigenvalue in **5** than in (**4**) (see also Figure 4) suggests that the paramagnetic part is larger in the former than in the latter.

TABLE 4: *X* Eigenvalues and the Corresponding Isotropic Shielding Constant (in ppm) in Compounds 4 and 5[a]

	X	Iso.	$CH_3(\beta)$
4	304.8	319.8	
5	257.7	289.1	30.7

[a] The difference between the isotropic values defines the methyl−β substituent effect.

TABLE 5: Four Relevant Energy Gaps for Defining the *X* Eigenvalue of the $\vec{\sigma}(^{17}O)$ Tensor in 4 and 5 (in Hartrees)[a]

energy gap		**4**	**5**
Δ(**6**)	$(C_1-O)^*$-$LP_1(O)$	0.862	0.866
Δ(**7**)	$(C_2-O)^*$-$LP_1(O)$	0.862	0.855
Δ(**8**)	$(C_1-O)^*$-(C_2-O)	1.103	1.100
Δ(**9**)	$(C_2-O)^*$-(C1−O)	1.103	1.093

[a] C_1 and C_2 the methyl and ethyl carbon atoms bonded to O.

In Table 5 are displayed the relevant energy gaps necessary to rationalize the *X* eigenvalues of the $\vec{\sigma}(^{17}O)$ magnetic shielding tensor in compounds **4** and **5** (Table 4). It is observed that energy gaps Δ(**7**) and Δ(**9**) corresponding to **5** are smaller than in **4**, corresponding to larger, in absolute value, contributions to the paramagnetic part of $\vec{\sigma}(^{17}O)$. It is observed that both of them involve the $(C_2-O)^*$ antibonding orbital, corresponding, in **5**, to the ethyl carbon atom bonded to O. Such a trend is in line with the larger *X* eigenvalue in **5** than in **4**.

It is noted that the calculated methyl−β substituent effect on $\sigma(^{17}O)$ in dimethyl ether displayed in Table 4 is in excellent agreement with the experimental value, 30 ppm.[27] As shown in Table 4, the difference in *X* eigenvalues is 47.1 ppm, yielding a contribution of 15.7 ppm to the methyl−β substituent effect. This indicates that such an effect has a strong contribution in changes of energy gaps involving the (C−O)* antibonding orbital that corresponds to the ethyl C−O bond. This effect is typical of the inductive effect when an H atom is replaced by a carbon atom.

c. Long-Range Substituent Effects. Aromatic Compounds. When a substituent is placed (Figure 7) several bonds away from the atom whose magnetic shielding constant, σ(M), is studied, then the qualitative analysis described above is much simplified because the inductive effect decays rapidly with the number of bonds separating them, and therefore the substituent effect is mainly defined by conjugative or hyperconjugative interactions.

For instance, in anisole $\sigma(^{17}O) = 48$ ppm, in *p*-OCH_3-anisole $\sigma(^{17}O)$ is 38 ppm, and in *p*-NO_2-anisole $\sigma(^{17}O)$ is 67 ppm (experimental values referenced to external water, taken from ref 28), Table 6. These values indicate that in anisole the conjugative interaction between the methoxy oxygen π-lone pair and the aromatic π-system yields a deshielding effect on $\sigma(^{17}O)$. It is known that OCH_3 is a resonance electron donor group and

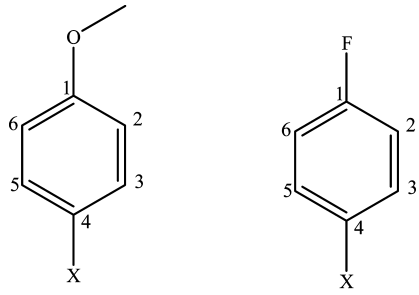

6 7

Figure 7. Para-substituted anisoles **6** and para-substituted fluorobenzenes **7**.

TABLE 6: ^{17}O Chemical Shifts for Anisole Derivatives 6 and for ^{19}F Chemical Shifts for Fluorobenzene Derivatives 7

	X	OCH_3	H	NO_2
6	$\delta(^{17}O)^a$	38	48	67
7	$\delta(^{19}F)^b$	−125.2	−113.8	−103.6

[a] Referenced to external water; taken from ref 28. [b] Referenced to $CFCl_3$; taken from ref 29.

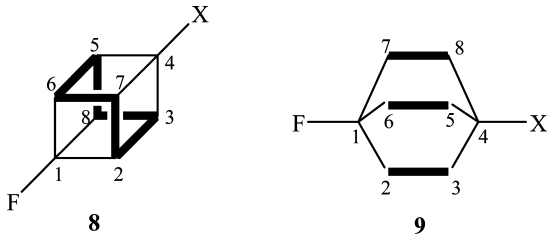

Figure 8. Pictorial representation of σ_{C-C} bonds hyperconjugating with σ^*_{C1-F} and σ^*_{C4-X} antibonding orbitals. When X is an axial substituent, both compounds have a 3-fold symmetry axis. Two points must be stressed: on one hand, in **8** there are six equivalent interactions, while in **9**, there are only three. On the other hand, such interactions are stronger in **8** than in **9**, because the substrate in the former is more strained than in the latter.

the larger the conjugative effect, the shorter the σ_{C1-O} bond length and, consequently, the better electron acceptor is its σ^*_{C1-O} antibonding orbital. This means that the lower the σ^*_{C1-O} antibonding orbital energy, the larger the conjugative effect between the methoxy group and the aromatic ring. One of the principal axes of the $\bar{\sigma}(^{17}O)$ tensor is perpendicular to the molecular plane, the Z axis, and the largest effect on its paramagnetic part originates from the 90° rotation of $LP_1(O)$, overlapping with the σ^*_{C1-O} antibonding orbital. This contribution is larger (in absolute value) the larger the conjugative effect with the aromatic ring, because the relevant energy gap is reduced. Similar rationalization is found for $\sigma(F)$ in para-substituted fluorobenzenes (Figure 7), where the para-substituent effect on $\sigma(F)$ is defined by the conjugative interaction between the π-fluorine lone pair, $LP_3(F)$, and the π-aromatic system,[29] Table 6. This interaction shortens the C_1-F bond length, and therefore this effect is similar to that described above for the methoxy group in para-substituted anisoles.

d. Long-Range Substituent Effects. Saturated Compounds. As a final example of the versatility of the qualitative approach discussed in this work, in this section it is shown how easy it is to rationalize the differences in ^{19}F SCSs in 1-F-4-X-cubane (**8**) and in 1-F-4-X-bicyclo[2.2.2]octane (**9**), Figure 8.

In these systems, **8** and **9**, the different efficiencies for transmitting the Fermi contact term of $^4J_{FC4}$ spin−spin couplings were recently discussed,[30] Figure 8, where bonds hyperconjugating with σ^*_{C-F} and σ^*_{C-X} are highlighted. Experimental couplings are as follows: in **8** $^4J(C_4,F)$ is 13.5 Hz,[31] while in **9** $^4J(C_4,F)$ is only 3.3 Hz.[32] These features make these two compounds excellent examples for applying the qualitative approach mentioned above in order to rationalize the different ^{19}F SCSs in both types of compounds. As an example, only X = Cl is examined because this is a typical substituent, and in this way, all four compounds quoted in Table 7 have a 3-fold symmetry axis. The respective experimental values (Table 7) are as follows: Cl-SCS on $^{19}F = -2.62$ ppm in **8**[31] and − 6.60 ppm in **9**.[33]

TABLE 7: Relevant NBO Parameters (calculated at the B3LYP-6-311G level) for Compounds 8 and 9 with X = H and Cl**

compounds	$\sigma_{C2-C3}\rightarrow\sigma^*_{C1-F}{}^a$	occupied $\sigma^*_{C-F}{}^b$	SCS $\delta(^{19}F)^c$
8(X = H)	4.1	67	0.0
8(X = Cl)	4.0	63	−2.62[d]
9(X = H)	3.6	56	0.0
9(X = Cl)	3.5	32	−6.60[e]

[a] In kcal/mol. [b] Antibonding occupation in 10^{-3}. [c] In ppm. [d] Taken from ref 31. [e] Taken from ref 33.

Owing to the strained σ_{C-C} bonds of type σ_{C2-C3} in **8**, interactions of type $\sigma_{C2-C3}\rightarrow\sigma^*_{C1-F}$ are stronger than similar interactions in **9**. Nonetheless, the differences of such interactions for X = H and for X = Cl are approximately the same. However, in compounds of type **8** there are six such interactions, while in **9** there are only three. This is the reason why the σ^*_{C-F} occupancies for X = H and X = Cl are so different for **8** and **9**. The notably smaller occupancy in **9**(X = Cl) than in **9**(X = H) indicates that the paramagnetic contribution to $\sigma(^{19}F)$ in the former is smaller, in absolute value, than in the latter, as observed experimentally.

4. Concluding Remarks

In this article a qualitative analysis of factors affecting the paramagnetic part of the nuclear magnetic shielding tensor is presented. The formulation of this approach is based on the following grounds. The influence of different inter- or intramolecular interactions on a second-order property can be qualitatively predicted if it can be known how they affect the main virtual excitations entering into that second-order property when its calculation is based on the Hartree−Fock method. Insight into such effects is achieved considering a set of consistent approximations, which are introduced into a second-order expression of the paramagnetic part of the nuclear magnetic shielding tensor.

A few examples are discussed where, for instance, it is concluded that the methyl−β-substituent effect on both ^{15}N and ^{17}O magnetic shielding constants is rationalized as originating in the inductive substituent effect. In many cases, for long-range substituent effects, this qualitative analysis is more straightforwardly applied because in this case, substituent effects on magnetic shielding constants originated mainly in changes of conjugative or hyperconjugative effects. Examples of these two cases are presented and results are more easily rationalized as described in section 3d.

Acknowledgment. C.F.T. is grateful to FAPESP (grant 06/03980-2, 08/06282-0) for the financial support of this work and to CNPq for fellowships. R.H.C. gratefully acknowledges financial support from CONICET (PIP 5119/05) and UBACYT(X047).

References and Notes

(1) (a) Karplus, M.; Pople, J. A. *J. Chem. Phys.* **1963**, *38*, 2802. (b) Kolker, H. J.; Karplus, M. *J. Chem. Phys.* **1963**, *39*, 2011. (c) Pople, J. A. *Mol. Phys.* **1964**, *7*, 301.

(2) Helgaker, T.; Jaszuñski, M.; Ruud, K. *Chem. Rev.* **1999**, *99*, 293.

(3) Jameson, C. J.; de Dios, A. C. Theoretical and physical aspects of nuclear shielding. Reported annually in *Nuclear Magnetic Resonance*; Webb, G. A., Ed.; The Royal Society of Chemistry: London, 2008; Vol. 37, p 51.

(4) (a) Barone, V.; Provasi, P. F.; Peralta, J. E.; Snyder, J. P.; Sauer, S. P. A.; Contreras, R. H. *J. Phys. Chem. A* **2003**, *107*, 4748. (b) Contreras, R. H.; Esteban, A. L.; Díez, E.; Della, E. W.; Lochert, I. J.; dos Santos, F. P.; Tormena, C. F. *J. Phys. Chem. A* **2006**, *110*, 4266.

(5) Oddershede, J. Polarization Propagator Calculations. In *Advances in Quantum Chemistry*; Academic: New York, 1978; Vol. 11, p 275.

(6) (a) Witanowski, M.; Stefaniak, L.; Szymañski, S.; Janusszewski, H. *J. Magn. Reson.* **1977**, *28*, 217. (b) Martin, G. J.; Dori, J.; Mechin, B. K. *Org. Magn. Reson.* **1979**, *12*, 229. (c) Duthaler, R. O.; Roberts, J. D. *J. Am. Chem. Soc.* **1978**, *100*, 3889. (d) Witanowski, M.; Stefaniak, L.; Webb, G. A. Nitrogen NMR Spectroscopy. In *Annual Reports in NMR Spectroscopy*; Webb, G. A., Ed.; Academic: London, 1986; Vol. 18, Table 12, p 246.

(7) (a) Crandall, J. K.; Centeno, M. A. *J. Org. Chem.* **1979**, *44*, 1183. (b) Delseth, C.; Kintzinger, J.-P. *Helv. Chim. Acta* **1978**, *44*, 1183. (c) Peralta, J. E.; Contreras, R. H.; Taurian, O. E.; Ortiz, F. S.; de Kowalewski, D. G.; Kowalewski, V. J. *Magn. Reson. Chem.* **1999**, *37*, 31. (d) Woodard, R. W. ^{17}O-NMR as a mechanistic probe to investigate chemical and bioorganic problems. In *^{17}O NMR Spectroscopy in Organic Chemistry*; Boykin, D. W., Ed.; CRC: Boca Raton, FL, 1990.

(8) (a) Ramsey, N. F. *Phys. Rev.* **1950**, *77*, 567. (b) Ramsey, N. F. *Phys. Rev.* **1950**, *78*, 699. (c) Ramsey, N. F. *Phys. Rev.* **1951**, *83*, 540. (d) Ramsey, N. F. *Phys. Rev.* **1952**, *86*, 243.

(9) Wolinski, K.; Hinton, J. F.; Pulay, P. *J. Am. Chem. Soc.* **1990**, *119*, 8251.

(10) (a) Geertsen, J. *Chem. Phys. Lett.* **1991**, *179*, 479. (b) Lazzeretti, P.; Malagoli, M.; Zanasi, R. *Chem. Phys. Lett.* **1994**, *220*, 299. (c) Ligabue, A.; Sauer, S. P. A.; Lazzeretti, P. *J. Chem. Phys.* **2003**, *118*, 6830.

(11) Frisch, M. J.; Trucks, G. W.; Schlegel, H. B.; Scuseria, G. E.; Robb, M. A.; Cheeseman, J. R.; Montgomery, J. A., Jr.; Vreven, T.; Kudin, K. N.; Burant, J. C.; Millam, J. M.; Iyengar, S. S.; Tomasi, J.; Barone, V.; Mennucci, B.; Cossi, M.; Scalmani, G.; Rega, N.; Petersson, G. A.; Nakatsuji, H.; Hada, M.; Ehara, M.; Toyota, K.; Fukuda, R.; Hasegawa, J.; Ishida, M.; Nakajima, T.; Honda, Y.; Kitao, O.; Nakai, H.; Klene, M.; Li, X.; Knox, J. E.; Hratchian, H. P.; Cross, J. B.; Bakken, V.; Adamo, C.; Jaramillo, J.; Gomperts, R.; Stratmann, R. E.; Yazyev, O.; Austin, A. J.; Cammi, R.; Pomelli, C.; Ochterski, J. W.; Ayala, P. Y.; Morokuma, K.; Voth, G. A.; Salvador, P.; Dannenberg, J. J.; Zakrzewski, V. G.; Dapprich, S.; Daniels, A. D.; Strain, M. C.; Farkas, O.; Malick, D. K.; Rabuck, A. D.; Raghavachari, K.; Foresman, J. B.; Ortiz, J. V.; Cui, Q.; Baboul, A. G.; Clifford, S.; Cioslowski, J.; Stefanov, B. B.; Liu, G.; Liashenko, A.; Piskorz, P.; Komaromi, I.; Martin, R. L.; Fox, D. J.; Keith, T.; Al-Laham, M. A.; Peng, C. Y.; Nanayakkara, A.; Challacombe, M.; Gill, P. M. W.; Johnson, B.; Chen, W.; Wong, M. W.; Gonzalez, C.; Pople, J. A. Gaussian 03 Revision C.02, Gaussian, Inc., Wallingford, CT, 2004.

(12) (a) Becke, A. D. *Phys. Rev. A* **1988**, *38*, 3098. (b) Becke, A. D. *J. Chem. Phys.* **1993**, *98*, 5648. (c) Lee, C.; Yang, W.; Parr, R. G. *Phys. Rev. B* **1988**, *37*, 785.

(13) (a) Glukhovstev, M. N.; Pross, A.; McGrath, M. P.; Radom, L. *J. Chem. Phys.* **1995**, *103*, 1878. (b) Krishnan, R.; Binkley, J. S.; Seeger, R.; Pople, J. A. *J. Chem. Phys.* **1980**, *72*, 650.

(14) (a) Schindler, M.; Kutzelnigg, W. *J. Chem. Phys.* **1982**, *76*, 1919. (b) Huzinaga, S.; Andzelm, J.; Klobukowsi, M.; Radzio-Andzelm, E.; Sakai, Y.; Tatewaki, H. *Gaussian Basis Sets for Molecular Calculations*; Elsevier: Amsterdam, 1984.

(15) Helgaker, T.; Watson, M.; Handy, N. C. *J. Chem. Phys.* **2000**, *113*, 9402.

(16) Angeli, C.; Bak, K. L.; Bakken, V.; Christiansen, O.; Cimiraglia, R.; Coriani, S.; Dahle, P.; Dalskov, E. K.; Enevoldsen, T.; Fernández, B.; Hättig, C.; Hald, K.; Halkier, A.; Heiberg H.; Helgaker, T.; Hettema, H.; Jensen, H. J. A.; Jonsson, D.; Jørgensen, P.; Kirpekar, S.; Klopper, W.; Kobayashi, R.; Koch, H.; Ligabue, A.; Lutnaes, O. B.; Mikkelsen, K. V.; Norman, P.; Olsen, J.; Packer, M. J.; Pedersen, T. B.; Rinkevicius, Z.; Rudberg, E.; Ruden, T. A.; Ruud, K.; Salek, P.; Sánchez de Merás, A.; Saue, T.; Sauer, S. P. A.; Schimmelpfennig, B.; Sylvester-Hvid, K. O.; Taylor, P. R.; Vahtras, O.; Wilson, D. J.; Ågren, H. Dalton, an Electronic Structure Program, Release 2.0, 2005. http://www.kjemi.uio.no/software/dalton/.

(17) Witanowski, M.; Stefaniak, L.; Webb, G. A. Nitrogen NMR Spectroscopy. In *Annual Reports in NMR Spectroscopy*; Webb, G. A., Ed.; Academic: New York, 1981; Vol. 11B, p 35.

(18) Díez, E.; Fabian, J. S.; Gerothanassis, I. P.; Esteban, A. L.; Abboud, J. L. M.; Contreras, R. H.; de Kowalewski, D. G. *J. Magn. Reson.* **1997**, *124*, 8.

(19) (a) Mertius, S.; Scrocco, E.; Tomasi, J. *J. Chem. Phys.* **1981**, *55*, 117. (b) Mertius, S.; Tomasi, J. *J. Chem. Phys.* **1982**, *65*, 239. (c) Cancs, M. T.; Mennucci, B.; Tomasi, J. *J. Chem. Phys.* **1997**, *107*, 3032. (d) Cossi, M.; Barone, V.; Mennuci, B.; Tomasi, J. *Chem. Phys. Lett.* **1998**, *286*, 253. (e) Mennucci, B.; Tomasi, J. *J. Chem. Phys.* **1997**, *106*, 5151.

(20) de Kowalewski, D. G.; Díez, E.; Esteban, A. L.; Barone, V.; Peralta, J. E.; Contreras, R. H. *Magn. Reson. Chem.* **2004**, *42*, 938.

(21) Tomasi, J.; Anil Kumar, P. G.; Fernández, I. *Chem. Rev.* **2005**, *105*, 2999.

(22) (a) Ferraro, M. B.; Natiello, M. A.; Contreras, R. H. *Int. J. Quantum Chem.* **1986**, *30*, 77. (b) Contreras, R. H.; Ruiz de Azúa, M. C.; Giriget, C. G.; Ferraro, M. B.; Diz, A. C. Análisis Químico-Cuántico de los parámetros de resonancia magnética nuclear. In *Nuevas Tendencias, Química Teórica*; Fraga, S., Ed.; Consejo Superior de Investigaciones Científicas: Madrid, 1989; Vol. II, Ch. VI. (c) Contreras, R. H.; Giribet, C. G.; Ruiz de Azúa, M. C.; Ferraro, M. B. Electronic Origin of NMR Parameters. *Studies in Physical and Theoretical Chemistry*; Fraga, S., Ed.; Elsevier: New York, 1992; Vol. 77(B), p 212.

(23) (a) Reed, A. E.; Curtiss, L. A.; Weinhold, F. *Chem. Rev.* **1988**, *88*, 899. (b) Weinhold, F. In *Encyclopedia of Computational Chemistry*; Schleyer, P. v. R., Ed.;Wiley: New York, 1998; Vol. 3, p 1792.

(24) Dewar, M. J. S.; Dougherty, R. C. *The PMO Theory of Organic Chemistry*; Plenum Press: New York, 1975.

(25) (a) Li, S.; Chestnut, D. B. *Magn. Reson. Chem.* **1985**, *23*, 625. (b) Li, S.; Chestnut, D. B. *Magn. Reson. Chem.* **1986**, *24*, 83. (c) Baumstark, A. L.; Boykin, D. W. In *^{17}O NMR Spectroscopy in Organic Chemistry*; Boykin, D. W., Ed.; CRC Press: Boca Raton, FL, 1990; Chapt. 4, p 69. (d) Gribble, G. W.; Keavy, D. J.; Olson, E. R.; Rae, I. D.; Staffa, A.; Herr, T. E.; Ferraro, M. B.; Contreras, R. H. *Magn. Reson. Chem.* **1991**, *29*, 422. (e) Facelli, J. C.; Contreras, R. H.; Tufró, M. F. *J. Mol. Struct. (THEOCHEM)* **1993**, *281*, 61. (f) Contreras, R. H.; Biekofsky, R. R.; Esteban, A. L.; Díez, E.; San Fabián, J. *Magn. Reson. Chem.* **1996**, *34*, 447.

(26) Orendt, A. M.; Biekofsky, R. R.; Pomilio, A. B.; Contreras, R. H.; Facelli, J. C. *J. Phys. Chem.* **1991**, *95*, 6179.

(27) Delseth, C.; Kintzinger, J.-P. *Helv. Chim. Acta* **1978**, *61*, 1327.

(28) Katoh, M.; Sugawara, T.; Kawada, Y.; Iwamura, H. *Bull. Chem. Soc. Jpn.* **1979**, *52*, 3475.

(29) Fifolt, M. J.; Sojka, S. A.; Wolfe, R. A.; Hojnicki, D. S. *J. Org. Chem.* **1989**, *54*, 3019.

(30) Contreras, R. H.; Esteban, A. L.; Díez, E.; Head, N. J.; Della, E. W. *Mol. Phys.* **2006**, *104*, 485.

(31) Della, E. W.; Head, N. J. *J. Org. Chem.* **1995**, *60*, 5303.

(32) Gakh, Y. G.; Gakh, A. A.; Gronenborn, A. M. *Magn. Reson. Chem.* **2000**, *38*, 551.

(33) Adcock, W.; Peralta, J. E.; Contreras, R. H. *Magn. Reson. Chem.* **2003**, *41*, 503.

JP901926P